Electronic Supplementary Material (ESI) for New Journal of Chemistry.

One step solvothermal synthesis of Carbon doped TiO_2-MoS_2 heterostructure composites with improved visible light catalytic activity

Mohamed Mukthar Ali[a] and Karunakaran Nair Yesodha Sandhya[a, *]

Supplementary Information

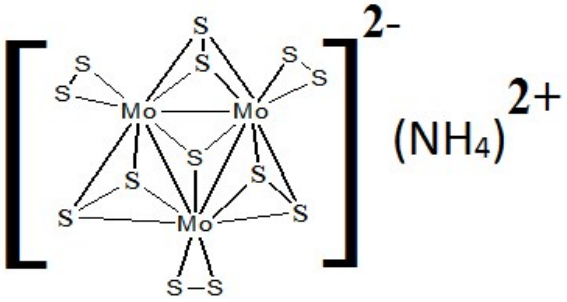

Fig. S1. Structure of the precursor molybdenum-sulphur cluster

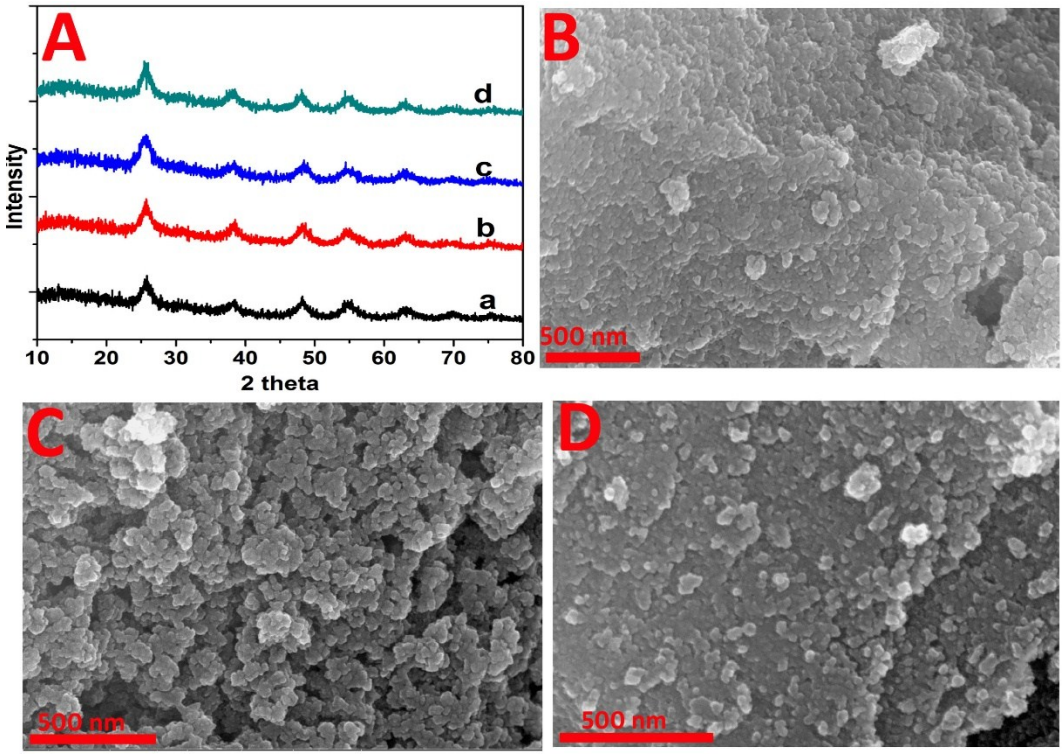

Fig. S2. (A): XRD patterns of (a) Control TiO_2; (b) C-TiO_2-$MoS_2$0.7; (c): C-TiO_2-$MoS_2$1.5and (d): C-TiO_2-$MoS_2$2.2 and SEM images of C-TiO_2-MoS_2 composites with (B): 0.4% (C): 1.5% and (D): 2.2% of MoS_2 loading.

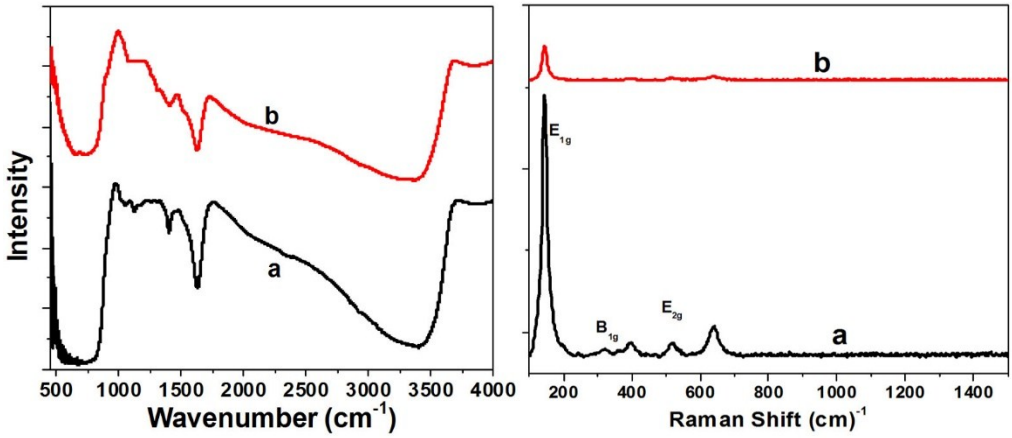

Fig. S3. Raman spectra of (a): Control TiO_2 and (b): C-TiO_2-MoS_2 0.7%

The Raman spectral analysis shows the peaks corresponding to TiO_2 anatase (Fig. 2B). The prominent peaks are 147, 400, 515 and 642 cm^{-1} corresponding to E_{1g}, B_{1g}, A_{1g}+B_{1g} and E_{2g} modes of anatase. There are no peaks observed for MoS_2 in the composite CTM0.7%. This can be probably due to the very low amount of MoS_2. E_{1g} and E_{2g} are mainly caused by symmetric stretching vibration of O-Ti-O in TiO_2 the B_{1g} peak was due to symmetric bending vibration of O-Ti-O bond while A_{1g} was caused by symmetric bending vibration of O-Ti-O [Tian et al. J. *Phys. Chem. C*, 2012, **116**, 7515−7519]. The decreased intensity of these peaks composites can be its interaction with MoS_2 nanosheets.

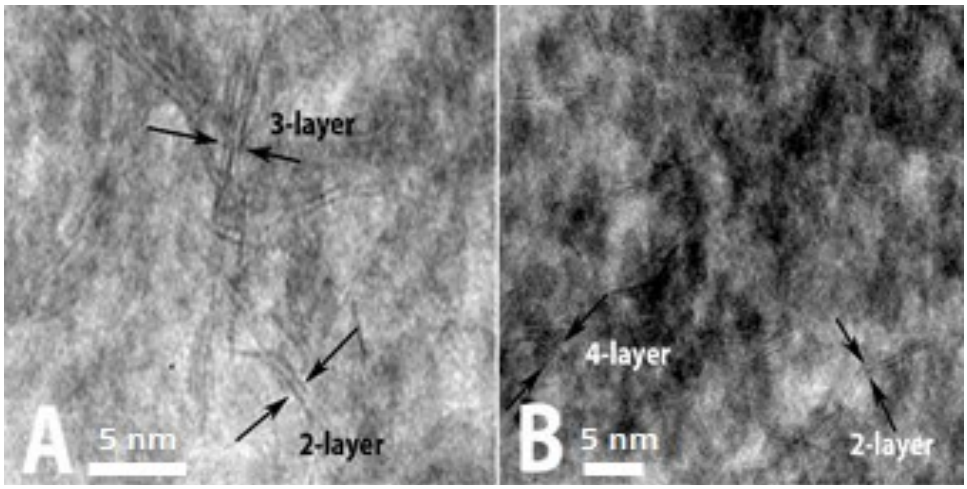

Fig. S4. HRTEM images of C-TiO_2-MoS_2 0.7% indicating the number of layers of MoS_2.

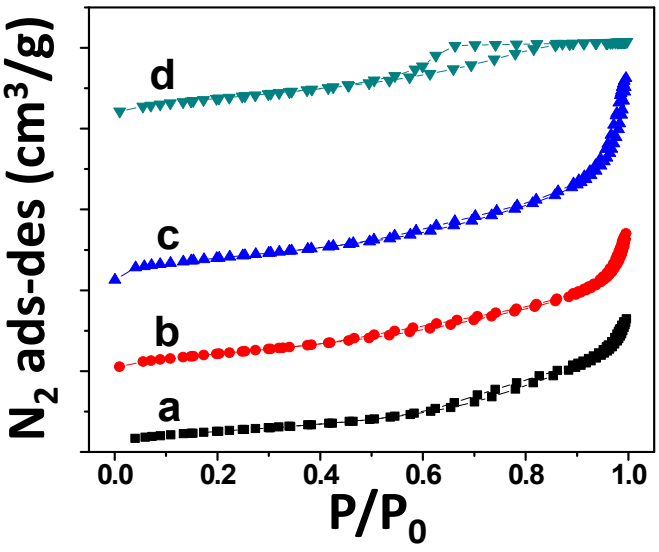

Fig. S5. N_2 adsorption-desorption isotherms of (a): Control TiO_2; (b): TiO_2-$MoS_2$0.7; (c): TiO_2-$MoS_2$1.5 and (d): TiO_2-$MoS_2$2.2 at 77K using liquid N_2.

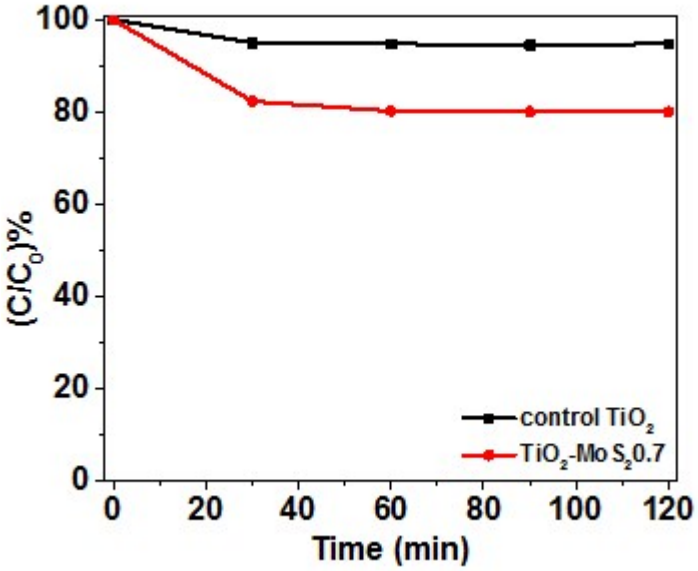

Fig. S6. Equilibrium adsorption of RhB with control TiO_2 and TiO_2-$MoS_2$0.7 composites up to 2 hrs.

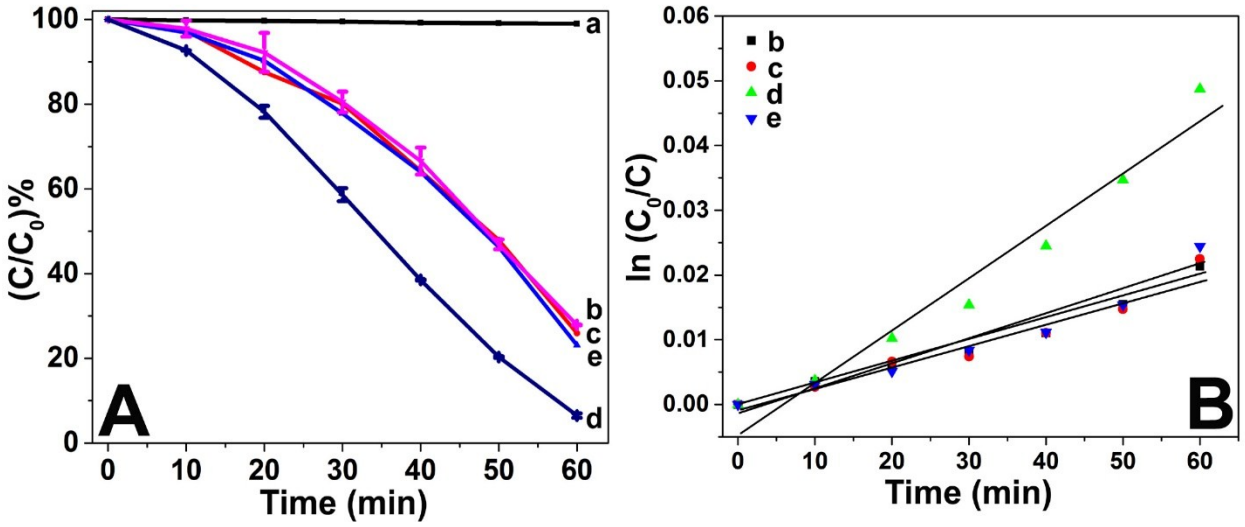

Fig. S7. (A) Visible light PD alone and (B) Rate constant plots of RhB for (a): No catalyst; (b): control TiO_2; (c): C-TiO_2-$MoS_2$0.24; (d): C-TiO_2-$MoS_2$0.7 and (e): C-TiO_2-$MoS_2$1.5 respectively.

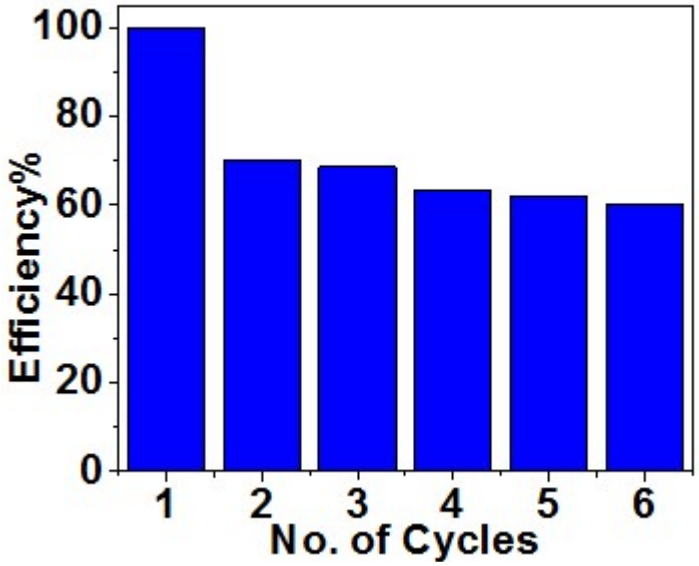

Fig. S8. Recycling studies in the visible light photodegradation of RhB by C-TiO_2-$MoS_2$0.7 composite.

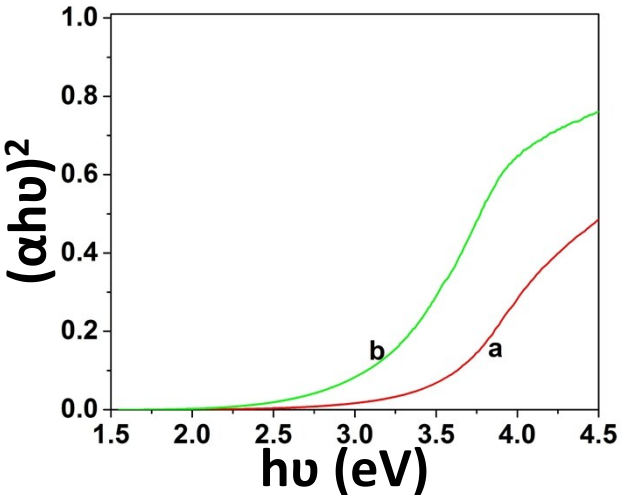

Fig. S9. Tauc plots of (a): control TiO_2 and (b): C-TiO_2-MoS_2 0.7

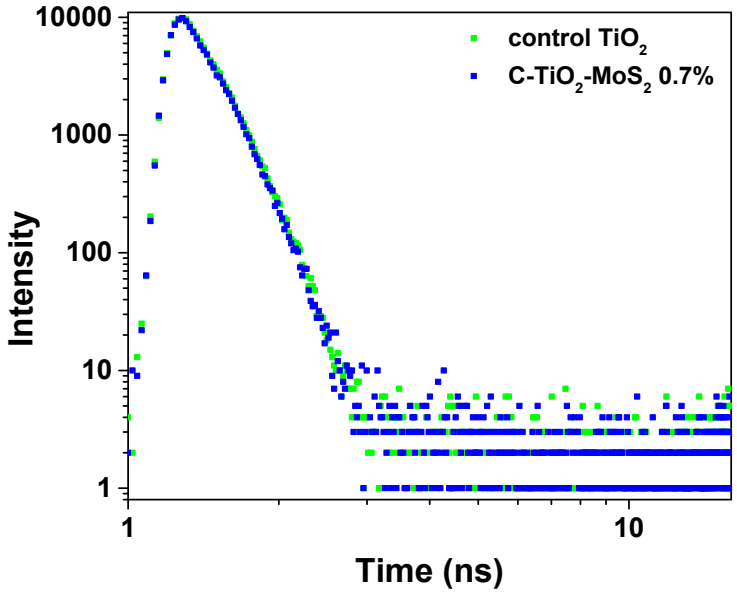

Fig S10. PL decay fit for RhB with control TiO_2 and C-TiO_2-MoS_2 0.7 with emission at 580 nm.

Table S1. BET Surface area, pore volume and pore sizes of catalysts.

Sample	**BET SA (m^2/g)**	**Pore volume (cm^3/g)**	**Pore area (nm)**
Control TiO_2	191	0.497	9.2
C-TIO_2-$MoS_2$0.7	274	0.549	8.2
C-TIO_2-$MoS_2$1.5	290	0.813	10.6
C-TIO_2-$MoS_2$2.2	261	0.325	4.9